

Local piezoelectric effect on single crystal ZnO microbelt transverse I-V characteristics

M. Li,¹ Y. J. Su,¹ W. Y. Chu,¹ L. J. Qiao,^{1,a)} Alex A. Volinsky,² and Grygoriy Kravchenko²

¹*Corrosion and Protection Center, Key Laboratory for Environmental Fracture (MOE), University*

of Science and Technology Beijing, Beijing 100083, People's Republic of China

²*Department of Mechanical Engineering, University of South Florida, Tampa, Florida 33620, USA*

(Received 11 November 2010; accepted 26 January 2011; published online 22 February 2011)

One-dimensional ZnO microbelts were prepared by chemical vapor deposition on Si substrates with sputtered Pt film. Using Pt-coated atomic force microscope (AFM) tip, the belts' transverse I-V characteristics were measured under varying applied elastic loads. ZnO microbelt conductivity reduced with load, but gradually increased upon unloading. Transverse electrical conductivity decrease at higher loads is attributed to the depletion zone formation induced by local piezoelectric effect in ZnO single crystal belt with $(000\bar{1})$ top surface indented by the AFM tip. The observed effect can be utilized in a nanoforce sensor device. © 2011 American Institute of Physics.

[doi:10.1063/1.3555456]

One-dimensional ZnO nanowires and nanobelts have been widely used for fabricating electromechanical devices such as nanogenerators, field effect transistors (FETs), and gated diodes due to a combination of piezoelectric and semiconducting properties.^{1–7} When ZnO nanobelt is bent, electrons travel from compressed to tensile regions driven by generated electric field, suppressing in-plane electrical conductivity.⁸ The working principle of ZnO nanobelt piezoelectric FET and piezoelectric gated diode is based on the interference between the piezoelectric-generated electrons and those induced by the in-plane applied electric field. This kind of electromechanical device based on bent ZnO nanobelt requires high fabrication tolerances. For example, fixing nanobelt ends is quite complicated and is likely to contaminate its surface. However, conductive film acts as an electrode for a belt positioned on its surface and an atomic force microscope (AFM) tip can serve as a second electrode. Piezoelectric coefficient measurements of ZnO nanobelts on conductive surfaces by Wang *et al.* demonstrated piezoelectric effect in the transverse direction.^{8,9} With the development of multifunctional AFM, *in situ* measurements of electrical,⁵ magnetic,¹⁰ and piezoelectric properties of nano-materials affected by mechanical, electrical, temperature, etc. fields become more convenient. Using conductive AFM, it is possible to investigate nanobelt transverse conductive properties under mechanical loading exerted by the AFM tip.

Since ZnO nanobelt deforms locally when indented by AFM tip, it can generate internal electric field along compression direction due to piezoelectric effect. Since conductive tip deforming the microbelt also serves as the top electrode, even small increases in ZnO local elastic deformation induce electrons transfer that contributes to transverse current.

A sensor detecting small forces can be fabricated utilizing this effect, and on the contrary, current passing through the device can be manipulated by applying different mechanical forces. ZnO nanobelts are too light to be easily moved and curl on the substrate surface under contact mode AFM, but microbelts are more stable and are better suited for

in situ transverse electrical properties measurements.

ZnO single crystal microbelts were placed on Si substrates with sputtered Pt films. The microbelts' transverse I-V characteristics were measured under varying load applied by conductive AFM tip, which also allowed characterizing surface topography. Synthesis of ZnO microbelts was accomplished by thermal evaporation of zinc powder in Ar and water vapor mixture at 300 Torr with 50 SCCM (SCCM denotes cubic centimeter per minute at STP) flow rate.¹¹ Introducing water vapor is necessary because water adsorption plays an important role in further ZnO single crystal growth from nanoscale to microscale. Belt-like shapes of as-synthesized ZnO powders can be easily observed by optical microscopy. The belts' width ranges from several to tens of microns, while their length is between several hundreds of microns and a few millimeters. As-prepared ZnO powders were ultrasonically dispersed in ethanol and spread over Si wafer with 100 nm Pt sputtered film. Agilent 5500 AFM (Agilent, Santa Clara, CA, USA) was used to measure the microbelts' electromechanical properties. The schematic diagram of the experimental setup is shown in Fig. 1(a). The same Pt film as on the Si wafer was sputtered on the AFM tip to maintain symmetric Schottky barriers between the electrodes and the two ZnO microbelt surfaces.

ZnO microbelt topography was acquired in tapping mode AFM, and in Fig. 1(b) the belt is 5.7 μm wide, 200 nm thick. The microbelt appears to be relatively flat laying on the substrate surface, confirmed by multiple images taken along its length. Physical contact was established between the microbelt top surface and conductive tip applying mechanical force, allowing for the I-V curve measurements. Tip loading position can be selected within the ZnO microbelt topographical image range. Belt electrical properties change due to surface contaminant adsorption, in which case the tip was moved to a higher conductivity area. Figure 2 shows a series of transverse I-V curves obtained from the ZnO microbelt in Fig. 1(b) at different applied normal forces. Measured I-V curves indicate that a barrier exists between the belt and the Pt electrodes. Agilent 5500 current measurement range is between -10 and 10 nA, thus higher currents could not be measured when the actual current exceeded this range.

^{a)}Electronic mail: lqiao@ustb.edu.cn.

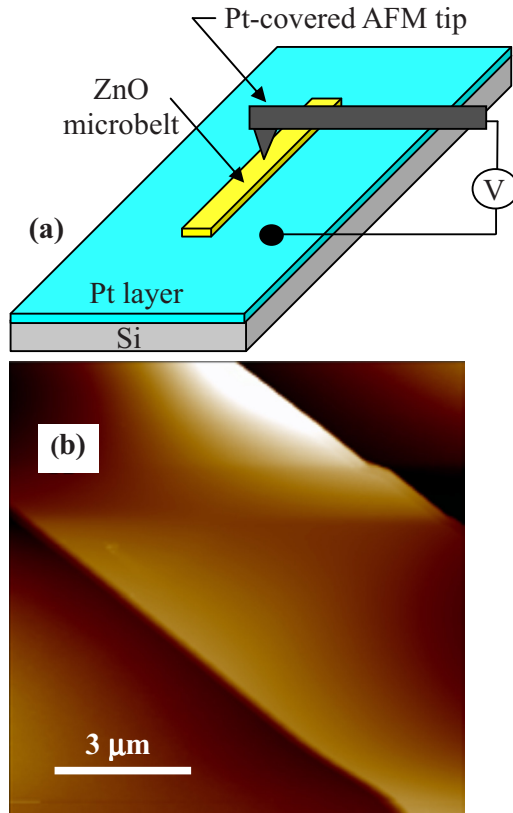


FIG. 1. (Color online) (a) Schematic diagram of the experimental setup. (b) AFM topography image of a single ZnO microbelt. Z scale is 300 nm.

ZnO microbelt exhibits good transverse electrical conductivity at 72 and 96 nN normal forces ($0.2 \Omega \text{ cm}$ specific resistance, comparable with $0.2\text{--}0.4 \Omega \text{ cm}$ measured for ZnO nanowires¹²); however, conductivity reduced rapidly with higher force. Eventually, this belt became an insulator when the force reached 190 nN at 1 V bias voltage (Fig. 2). The belt's transverse conductivity increases and recovers gradually upon tip withdrawal and force reduction. This behavior is completely reversible and repeatable when loading-unloading experiments are conducted at different locations on the microbelt surface. Mechanical force versus conductivity trend shows good repeatability in other five tested ZnO microbelts. In Fig. 3, ZnO microbelt resistance increases sig-

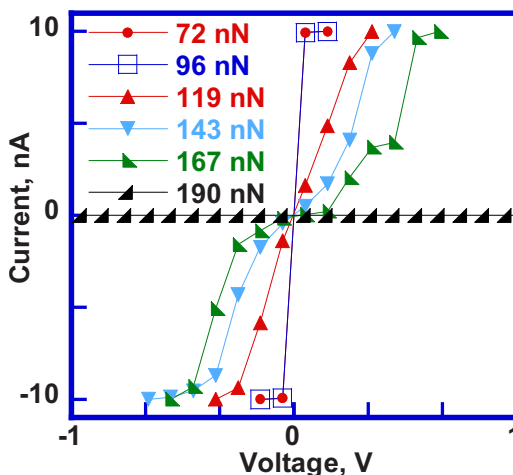


FIG. 2. (Color online) Transverse ZnO microbelt I-V characteristics at varying AFM tip load.

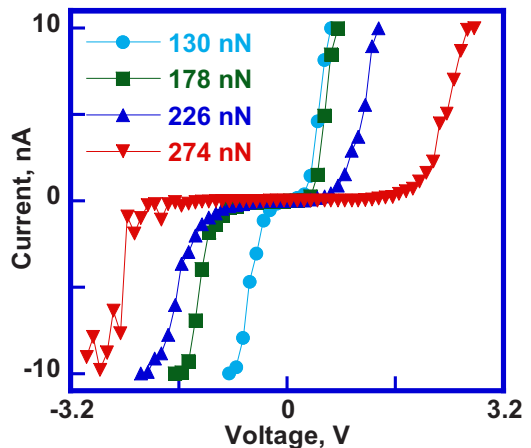


FIG. 3. (Color online) Transverse I-V characteristics of another ZnO microbelt at varying AFM tip load.

nificantly with the loading force ranging from 130 to 274 nN. Different from Fig. 2, I-V transverse characteristics of this belt exhibit nearly symmetric valve voltage behavior, related to the Schottky barriers between the semiconducting microbelt and the metal electrodes. At 274 nN load, the current is very low at 2 V applied voltage, but undergoes a rapid increase once the voltage exceeds 2 V. The difference in the valve voltage values at positive and negative voltages comes from the local piezoelectric effect occurring at the top indented surface.

Higher mechanical tip force corresponds to a larger contact area and better conductivity for most materials because of lower Schottky barrier. Consequently, the valve voltage should be lower; however, in experiments with piezoelectric ZnO microbelts, the valve voltage increases compared with the I-V curves acquired at lower loads, and the Schottky barrier is much higher at deeper indentations than at shallower indentations.

It should be noted that this current-load dependence was not exhibited by some other tested ZnO microbelts, ascribed to their different top surface crystal orientation. It is well known that the most common ZnO nanobelt growth direction is along the [0001] c-axis, [01 $\bar{1}$ 0] and [21 $\bar{1}$ 0] directions, with corresponding (0001) and (21 $\bar{1}$ 0) top surfaces.¹³ No piezoelectric characteristics are observed under normal stress for those belts lying on the (21 $\bar{1}$ 0) top surface,⁹ but things change when ZnO microbelts have (0001) or (0001 $\bar{1}$) top surface. ZnO surface is locally compressed when normal stress is applied. According to load-displacement curves obtained by nanoindentation performed on ZnO microbelts (Fig. 4) with Hysitron Triboindenter (Hysitron, USA), displacement pop-in event under load control, corresponding to emerging dislocations and plastic deformation, does not occur until 320 μm exerted by a Berkovich tip, with the stress level at least 2000 times higher than that applied by the AFM tip. Figure 4 also shows Hertzian elastic contact fit assuming 85 GPa ZnO microbelt reduced elastic modulus and 150 nm Berkovich indenter tip radius. This means that ZnO microbelt is definitely deformed elastically during AFM indentation experiments. The microbelts' (0001 $\bar{1}$) top surface is terminated by oxygen ions. Elastic strain leads to ZnO lattice compression along the [0001] direction, corresponding to the formation of build-up electric field induced by the piezoelec-

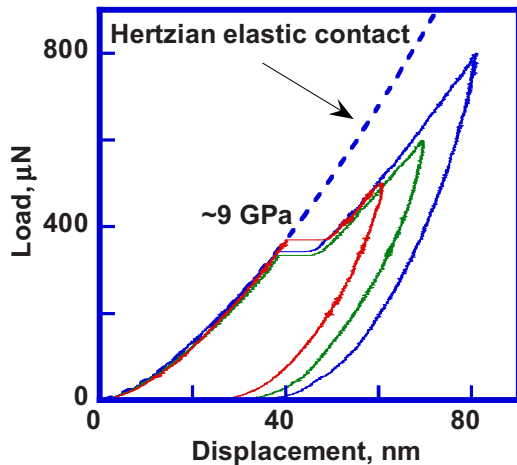


FIG. 4. (Color online) Load-displacement curves of ZnO microbelt using nanoindentation with Berkovich tip along with the Hertzian elastic contact fit. Pop-in happens at ~ 9 GPa normal stress.

tric effect, with negative charge on the indented surface, and positive charge in the microbelt bulk.¹⁴ In this paper, it is ZnO microbelt with $(000\bar{1})$ top surface that showed semiconducting and insulating properties as the depletion zone would not form unless loaded surface is negatively charged, because in an n-type semiconductor, charge carriers (electrons) move from negative to positive side. Piezoelectric FET mechanism proposed by Wang⁸ also suggests that the source and drain current changes due to ZnO nanowire bending are associated with carrier trapping effect and charge depletion zone created under elastic deformation. Commonly, build-up electric field is completely reversed when the belt is loaded in compression versus tension. Consequently, electrons in the deformation zone will transfer to the positive end, forming a depletion zone underneath the tip. This depletion zone acts as a barrier for the belt transverse conduction. Since a sharp AFM tip radius is 30 nm, and its contact area is smaller than the microbelt elastic deformation zone, all of the tip contact area is covered by the depletion region. Depletion region increases with load, and the barrier is higher, thus transverse current reduces with load. If the barrier is higher than the applied voltage between the two electrodes, the belt exhibits current cut-off behavior, which can be used to manipulate transverse current by changing the mechanical load. ZnO deformation under AFM tip is elastic, thus current will increase and recover to its original level if mechanical force is

gradually decreased, supported by experiments.

The observed current-load dependence was only exhibited by ZnO microbelts with $(000\bar{1})$ top surface. For other tested ZnO microbelts, transverse current increased with load slightly, largely affected by their top surface. For ZnO microbelts with $(2\bar{1}10)$ top surface, lattice compression direction is perpendicular to the $[0001]$ direction, and these microbelts do not exhibit piezoelectric effect upon indentation. Thus, there is no internal electric field formed in this case when ZnO is deformed, and its electrical conductivity does not decrease.

In summary, ZnO microbelts were fabricated using chemical vapor deposition in the presence of water vapor. Transverse current reduced with increasing load exerted by conductive AFM tip caused by piezoelectric effect in ZnO microbelts with $(000\bar{1})$ top surface. ZnO microbelt with $(000\bar{1})$ top surface can be used to fabricate nanoforce sensors and other nanoelectromechanical and microelectromechanical systems devices.

This work was supported by the National Natural Science Foundation of China under Grant Nos. 51072021 and 50632010. Beijing Municipal Commission of Education under Grant No. YB20091000801. A.A.V. acknowledges the support from the National Science Foundation under Grant No. 1000138.

- ¹J. H. He, C. L. Hsin, and Z. L. Wang, *Adv. Mater. (Weinheim, Ger.)* **19**, 781 (2007).
- ²Z. L. Wang and J. H. Song, *Science* **312**, 242 (2006).
- ³Y. W. Heo, L. C. Tien, D. P. Norton, B. S. Kang, F. Ren, B. P. Gila, and S. J. Pearton, *Appl. Phys. Lett.* **85**, 2002 (2004).
- ⁴M. P. Lu, J. H. Song, and M. Y. Lu, *Nano Lett.* **9**, 1223 (2009).
- ⁵Z. Y. Fan and J. G. Lu, *Appl. Phys. Lett.* **86**, 032111 (2005).
- ⁶W. I. Park, J. S. Kim, and G. C. Yia, *Appl. Phys. Lett.* **85**, 5052 (2004).
- ⁷Y. Yang, J. Qi, W. Guo, Y. Gu, Y. Huang, and Y. Zhang, *Phys. Chem. Chem. Phys.* **12**, 12415 (2010).
- ⁸X. D. Wang, J. Zhou, J. H. Song, J. Liu, N. S. Xu, and Z. L. Wang, *Nano Lett.* **6**(12), 2768 (2006).
- ⁹M. H. Zhao, Z. L. Wang, and S. X. Mao, *Nano Lett.* **4**, 587 (2004).
- ¹⁰D. Navas and A. Asenjo, *J. Magn. Magn. Mater.* **290–291**, 191 (2005).
- ¹¹Z. W. Pan, Z. R. Dai, and Z. L. Wang, *Science* **291**, 1947 (2001).
- ¹²S. W. Yoon, J. H. Seo, K.-H. Kim, J.-P. Ahn, T.-Y. Seong, K. B. Lee, and H. Kwon, *Thin Solid Films* **517**, 4003 (2009).
- ¹³Z. L. Wang, *Mater. Today* **7**, 26 (2004).
- ¹⁴J. H. Song, X. D. Wang, J. Liu, H. B. Liu, Y. L. Li, and Z. Lin Wang, *Nano Lett.* **8**(1), 203 (2008).